Geophysical Research Letters

RESEARCH LETTER
10.1029/2018GL081341

Special Section:
Carbon and Weather: Results from the Atmospheric Carbon and Transport – America Mission

Characterization of Regional-Scale CO_2 Transport Uncertainties in an Ensemble with Flow-Dependent Transport Errors

Hans W. Chen[1,2,3], Fuqing Zhang[1,2], Thomas Lauvaux[1,4], Kenneth J. Davis[1,5], Sha Feng[1], Martha P. Butler[1], and Richard B. Alley[6]

[1]Department of Meteorology and Atmospheric Science, The Pennsylvania State University, University Park, PA, USA, [2]Center for Advanced Data Assimilation and Predictability Techniques, The Pennsylvania State University, University Park, PA, USA, [3]Now at Department of Physical Geography and Ecosystem Science, Lund University, Lund, Sweden, [4]Now at Laboratoire des Sciences du Climat et de l'Environnement, CEA, CNRS, UVSQ/IPSL, Université Paris-Saclay, Orme des Merisiers, Gif-sur-Yvette, France, [5]Earth and Environmental Sciences Institute, The Pennsylvania State University, University Park, PA, USA, [6]Department of Geosciences, and Earth and Environmental Systems Institute, The Pennsylvania State University, University Park, PA, USA

Abstract Inference of CO_2 surface fluxes using atmospheric CO_2 observations in atmospheric inversions depends critically on accurate representation of atmospheric transport. Here we characterize regional-scale CO_2 transport uncertainties due to uncertainties in meteorological fields using a mesoscale atmospheric model and an ensemble of simulations with flow-dependent transport errors. During a 1-month summer period over North America, transport uncertainties yield an ensemble spread in instantaneous CO_2 at 100 m above ground level comparable to the CO_2 uncertainties resulting from 48% relative uncertainty in 3-hourly natural CO_2 fluxes. Temporal averaging reduces transport uncertainties but increases the influence of CO_2 uncertainties from the lateral boundaries. The influence of CO_2 background uncertainties is especially large for column-averaged CO_2. These results suggest that transport errors and CO_2 background errors limit regional atmospheric inversions at two distinct timescales and that the error characteristics of transport and background errors should guide the design of regional inversion systems.

Plain Language Summary Accurate estimates of regional-scale CO_2 surface fluxes are essential to improve our understanding of the carbon cycle and to verify human CO_2 emission inventories. CO_2 surface fluxes can be inferred from atmospheric CO_2 measurements through inversion methods, which use atmospheric transport models to relate CO_2 concentration to fluxes. However, previous studies have shown that inversion results can be sensitive to errors in the simulated atmospheric transport. To better understand how to account for such transport errors, we characterize the uncertainties in simulated CO_2 concentration due to uncertainties in atmospheric transport by running an ensemble of perturbed transport simulations in a regional atmospheric model. Our results show that CO_2 uncertainties due to transport uncertainties are about half the magnitude as uncertainties due to erroneous CO_2 surface fluxes while displaying similar spatial and temporal patterns. Transport uncertainties are reduced when CO_2 is time averaged, but at the same time the influence of uncertainties in the CO_2 background concentration is increased at longer timescales. Thus, the flux signals in regional inversions are degraded by transport errors and CO_2 background errors at different timescales, and it is imperative to properly account for these errors to obtain reliable regional-scale CO_2 flux estimates.

Key Points:
- We quantify CO_2 transport uncertainties due to uncertainties in meteorological fields at the regional scale and submonthly timescales
- Atmospheric CO_2 estimates that are strongly influenced by CO_2 surface fluxes tend to also have large transport uncertainties
- The signal-to-noise ratio in in situ CO_2 is limited by transport errors at subweekly timescales and CO_2 background errors at longer scales

Supporting Information:
- Supporting Information S1

Correspondence to:
F. Zhang,
fzhang@psu.edu

Citation:
Chen, H. W., Zhang, F., Lauvaux, T., Davis, K. J., Feng, S., Butler, M. P., & Alley, R. B. (2019).Characterization of regional-scale CO_2 transport uncertainties in an ensemble with flow-dependent transport errors. *Geophysical Research Letters*, *46*. https://doi.org/10.1029/2018GL081341

Received 15 NOV 2018
Accepted 19 MAR 2019
Accepted article online 25 MAR 2019

1. Introduction

Atmospheric CO_2 inversions provide a method to infer CO_2 surface fluxes from observed atmospheric CO_2 mole fractions through the use of an atmospheric transport model (Ciais et al., 2010; Enting, 2002) and have been widely employed to gain insights into the global and regional carbon cycle (e.g., Tans et al., 1990). Moreover, inversions can potentially provide critical independent verification of anthropogenic CO_2 emission inventories to support future climate agreements (National Research Council, 2010). However, there is still a considerable divergence between results of inversions at the continental scale (Chevallier et al., 2014; Gurney et al., 2002), which inhibits our ability to draw reliable conclusions about regional CO_2 sources and

sinks. Intercomparisons of inversion systems have revealed that the estimated CO_2 fluxes are often sensitive to the inversion setup (Gurney et al., 2002; Peylin et al., 2013). For example, the choice of atmospheric transport model can lead to contrasting conclusions about regional CO_2 fluxes (Stephens et al., 2007).

One of the largest sources of errors in atmospheric inversions is erroneous representation of atmospheric conditions by the atmospheric transport model (Gloor et al., 1999). Errors in atmospheric transport can lead to mismatches between modeled and observed CO_2 that are mistaken as flux signals. Despite the recognized importance of transport errors in atmospheric inversions, transport uncertainties are typically not fully accounted for in current inversion systems, to a large part because of a lack of complete understanding of the transport error characteristics. Transport uncertainties are typically prescribed and assumed to be uncorrelated in space and time. With denser observations, for example, from satellite measurements, it is expected that correlated transport errors will have a larger influence on inversion results (Chevallier et al., 2010).

Transport errors can be grossly divided into two components: (1) transport errors due to errors in the transport model, including errors in model parameters, and (2) transport errors due to errors in meteorological initial and boundary conditions. Previous studies have mostly focused on the first class of transport errors and quantified the uncertainties using different transport models (e.g., Engelen et al., 2002; Gurney et al., 2002) or perturbed model physics (e.g., Díaz-Isaac et al., 2018). However, even with a perfect transport model, there can exist significant transport errors due to errors in meteorological initial and boundary conditions combined with intrinsic atmospheric error growth. A few studies have quantified CO_2 transport uncertainties due to uncertainties in meteorological conditions at the global scale (Liu et al., 2011; Miller et al., 2015; Polavarapu et al., 2016) and the mesoscale (Lauvaux et al., 2009) and investigated ways to include transport uncertainties in atmospheric inversions (Kang et al., 2012; Lin & Gerbig, 2005), but no rigorous characterization of CO_2 uncertainties due to flow-dependent transport errors has been performed at the regional to continental scales.

In this paper we characterize transport uncertainties due to uncertainties in meteorological initial and boundary conditions on subseasonal timescales. We focus on a summer case during the month of July 2016 over North America, coincident with the first intensive Atmospheric Carbon and Transport (ACT)-America field campaign. ACT-America's objectives include quantifying and reducing uncertainties in atmospheric inverse estimates of CO_2 fluxes via targeted comparisons of simulations and aircraft observations of atmospheric CO_2 mole fractions. This paper represents a preliminary exploration of the uncertainties in atmospheric CO_2 mole fractions associated with transport uncertainty. Through the use of an ensemble data assimilation system, the flow-dependent forecast error structures are represented by an ensemble of high-resolution model simulations and constrained by periodically assimilating simulated rawinsonde observations. To put the transport uncertainties in perspective, we performed two additional sensitivity experiments, one in which we perturbed only CO_2 surface fluxes and the other in which we perturbed only CO_2 lateral boundary conditions. Together, these three experiments shed light on how flux signals in atmospheric CO_2 mole fractions are degraded in regional inversions by uncertainties in atmospheric transport and CO_2 lateral boundary conditions.

2. Methods

2.1. Model and Data

We use the Weather Research and Forecasting (WRF) model coupled with Chemistry (WRF-Chem; Grell et al., 2005) version 3.6.1, which is a regional chemical transport model with online meteorology from WRF. WRF is a fully compressible, nonhydrostatic mesoscale model integrated on the staggered Arakawa C-grid and with mass-based terrain-following vertical model levels (Skamarock et al., 2008). Here WRF-Chem was run at a horizontal resolution of 27 km in a domain that covers most of North America (see Figure 1) and with 60 vertical levels extending up to 50 hPa. The vertical spacing is smallest in the boundary layer and increases gradually with height.

CO_2 is treated as an inert passive tracer; that is, the trace gas has no feedback on meteorological variables and is not part of any chemical reactions. Thus, the total mass of CO_2 in the model domain depends only on the surface fluxes of CO_2 inside the domain and the CO_2 lateral boundary conditions. We use a positive definite sixth-order diffusion scheme to more accurately simulate diffusive processes, the Mellor-Yamada

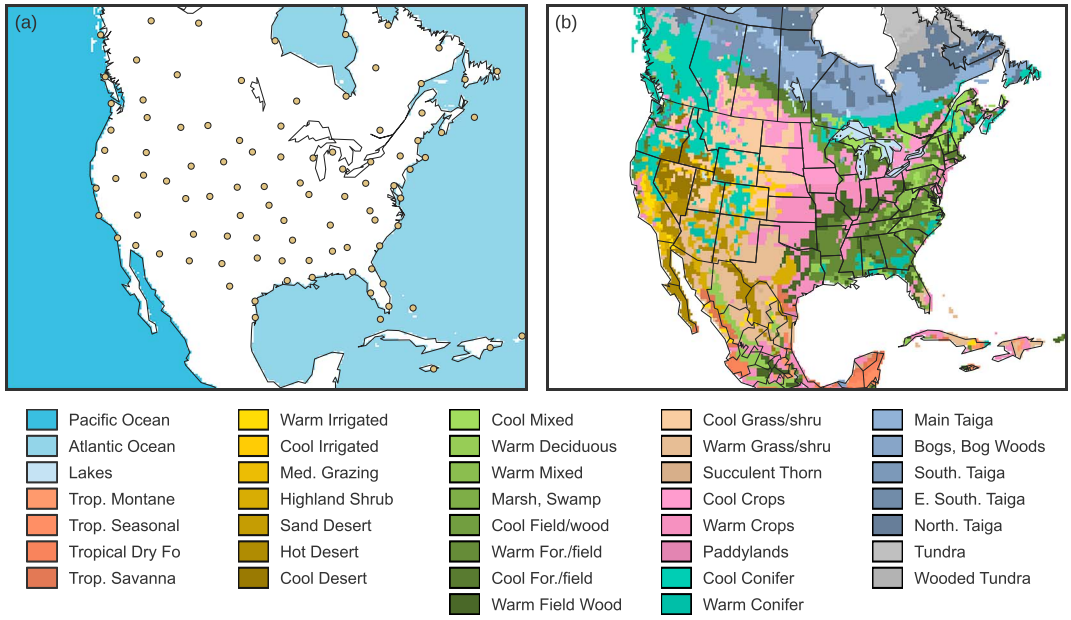

Figure 1. (a) Map of the model domain and locations of simulated rawinsonde observations (yellow circles) that were used to constrain transport errors. The shading shows the ocean regions that were used to perturb oceanic CO_2 fluxes. (b) Ecoregions and lakes used in the terrestrial CO_2 flux perturbations (shading), based on the ecoregions defined by Olson et al. (1985; doi: 10.3334/CDIAC/lue.ndp017).

Nakanishi and Niino Level 2.5 PBL scheme (Nakanishi & Niino, 2006), to represent the planetary boundary layer physics, and the Kain-Fritsch convective scheme (Kain, 2004). See supporting information section S1 (Dudhia, 1988; Hong et al., 2004; Mlawer et al., 1997; Tewari et al., 2004) for more information about the WRF-Chem setup.

WRF-Chem was initialized using meteorological initial conditions from the global European Centre for Medium-Range Weather Forecasts Interim Reanalysis (ERA-Interim; Dee et al., 2011) and driven by boundary conditions from ERA-Interim available at 6-hr intervals. For CO_2 mole fractions and surface fluxes, we used the CarbonTracker Near-Real Time (CT-NRT) v2017 reanalysis (https://www.esrl.noaa.gov/gmd/ccgg/carbontracker/CT-NRT/), which is provided by the National Oceanic and Atmospheric Administration. CT-NRT is an extension of the CarbonTracker system (Peters et al., 2007) and uses observations of atmospheric CO_2 to optimize CO_2 surface fluxes. Here we used the global CT-NRT product with a spatial resolution of $3 \times 2°$ longitude-latitude and 25 vertical levels for atmospheric CO_2 mole fractions, a spatial resolution of $1 \times 1°$ longitude-latitude for surface CO_2 fluxes, and 3-hourly time resolution for both CO_2 mole fractions and fluxes. To simplify the interpretation of the results, we chose to focus on land biosphere and ocean fluxes and excluded emissions from fossil fuel combustion and wildfire. The latter two sources are often assumed to be relatively well-known in inversions (e.g., CarbonTracker and CT-NRT; ; Peters et al., 2007) and therefore not considered in the flux optimization.

2.2. Experiments

As noted above we performed three experiments for the month of July 2016, independently perturbing meteorological fields in the first (labeled "Transport" below), perturbing surface CO_2 fluxes in the second ("Flux"), and perturbing CO_2 lateral boundary conditions in the third ("Background"). These experiments are explained next.

For the Transport sensitivity experiment, we performed an observing system simulation experiment to quantify the effect of meteorological uncertainties on atmospheric CO_2 mole fractions. In the observing system simulation experiment, we assume that the transport model is perfect and that the CO_2 initial conditions, lateral boundary conditions, and surface fluxes are known; thus, errors in CO_2 mole fractions arise only from uncertainties in meteorological initial and boundary conditions. These errors are characterized using an ensemble of 40 WRF-Chem forecasts with flow-dependent transport errors, which was constructed following the methodology of Meng and Zhang (2007). First, we perturbed the meteorological initial conditions at

0 UTC on 1 July 2016 using climatological background error statistics (supporting information section S2) to generate 41 ensemble members. The 41st member was taken as the "truth" and run forward in free forecast mode for 1 month to create a reference run. Atmospheric errors tend to grow rapidly with time (Lorenz, 1963), so to constrain the magnitude of transport errors in the other 40 ensemble members, we extracted pseudo-rawinsonde observations from the reference run with realistic added measurement noise (supporting information Figure S1) and assimilated them into the other members every 12 hr using the ensemble Kalman filter (Evensen, 1994; Houtekamer & Zhang, 2016). This study employed the Penn State University WRF-ensemble Kalman filter system, which is originally developed in Meng and Zhang (2008a, 2008b), but whose configuration and algorithms have been continuously updated and improved for a wide range of applications (e.g., Weng & Zhang, 2012, 2016; Zhang et al., 2016, 2019, 2011, 2009); see also supporting information section S2 (Gaspari & Cohn, 1999; Zhang et al., 2004). The locations of the rawinsonde observations are based on the operational network from the Meteorological Assimilation Data Ingest System and are shown in Figure 1a. All ensemble members in this experiment were initialized with identical CO_2 initial conditions and forced with the same CO_2 lateral boundary conditions and surface fluxes. This ensemble-based data assimilation approach allows us to explicitly model transport error structures and estimate transport error magnitudes based on the current meteorological observation network.

To quantify the sensitivity of atmospheric CO_2 mole fractions to CO_2 surface fluxes, we performed another sensitivity experiment (Flux) in which only the CO_2 fluxes were perturbed using an approach typically found in CO_2 inversions. Specifically, we followed the methodology of the CarbonTracker system (Peters et al., 2007): for each predefined subregion, a random scaling factor is drawn from a Gaussian distribution with mean 1 and standard deviation 0.4 (40% relative uncertainties) for ocean subregions (Figure 1a) and 0.8 (80% relative uncertainties) for land subregions (Figure 1b) and applied to the 3-hourly fluxes from CT-NRT in the subregion. Flux errors are assumed to be uncorrelated between different subregions. Unlike CarbonTracker, we do not optimize the scaling factors but instead keep them constant for the whole simulation period. Forty flux realizations were generated using this method and propagated to atmospheric CO_2 mole fractions through the true transport from the reference run.

Regional CO_2 inversions also need to consider background CO_2 mole fractions that originate from outside the regional domain. In the third and final sensitivity experiment (Background), we assessed the uncertainties in atmospheric CO_2 mole fractions stemming from uncertainties in the CO_2 background using four ensemble members driven by lateral boundary conditions from four different global CO_2 models: CarbonTracker CT2016 ($3 \times 2°$ lon-lat, 25 vertical levels; Peters et al., 2007), with updates documented (http://carbontracker.noaa.gov); CMS-Flux GEOS-Chem ($5 \times 4°$ lon-lat, 47 vertical levels; Liu et al., 2014); TM5 4DVAR ($3 \times 2°$ lon-lat, 25 vertical levels; Basu et al., 2016); and GEOS-Chem-CarbonTracker ($5 \times 4°$ lon-lat, 47 vertical levels; Schuh et al., 2015). We used 3-hourly resolution output from all global models and the fluxes in all members were set to 0. One caveat of this experiment is that we used data from 2010 instead of 2016 because that was the last year for which all products were available to us when this study was conducted. This point is not critical for our study because we are interested in the uncertainties (i.e., the resulting ensemble spread) rather than the actual CO_2 mole fractions and focus on error statistics and orders of magnitudes. As in the flux sensitivity experiment, the background sensitivity simulations were run using the true transport from the reference run. To include uncertainties in CO_2 initial conditions in the Background experiment, we started the simulations in this experiment from December the previous year to allow time for the lateral boundary CO_2 to completely fill the domain.

These three experiments quantify the sensitivity of atmospheric CO_2 mole fractions to uncertainties in transport, CO_2 surface fluxes, and CO_2 background mole fractions. Unless otherwise noted, all uncertainties are reported in terms of one ensemble standard deviation in CO_2 mole fractions of all simulations in each experiment. Whenever uncertainties were integrated in space or time, we averaged the squared ensemble standard deviations (i.e., the variances) and then took the square root of the average.

3. Results and Discussion

Atmospheric transport errors were constrained in the data assimilation system to about 2.2 m/s for the instantaneous u and v components of the wind in terms of vertically and domain-integrated

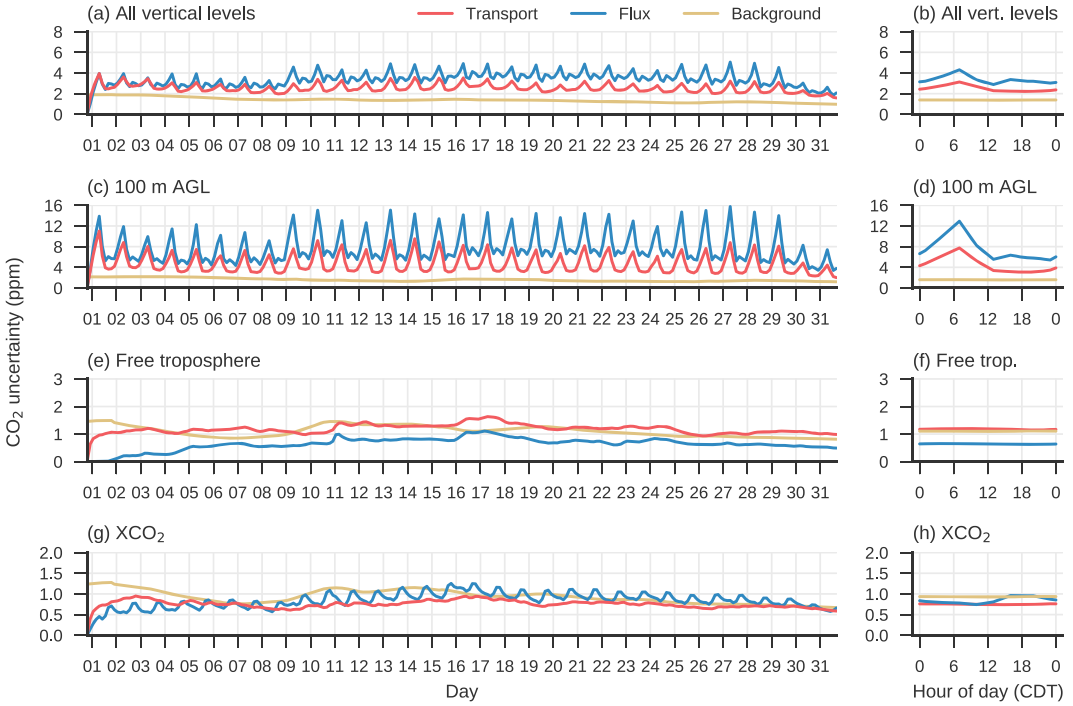

Figure 2. Time evolution of 3-hourly domain-integrated uncertainties in CO_2 mole fractions in terms of one ensemble standard deviation in the different experiments for (a, b) all vertical model levels (no vertical averaging), (c, d) CO_2 at 100 m above ground level (AGL), (e, f) CO_2 in the free troposphere, and (g, h) column-averaged CO_2. The right column shows the corresponding mean diurnal cycles for the different error components in Central Daylight Time (CDT), which is the local time zone for the middle of the domain.

root-mean-square errors between the mean of the ensemble simulations and the reference run (supporting information Figure S2). Although the ensemble simulations and the reference run use the same boundary layer parameterization scheme, there are significant errors in boundary layer height due to uncertainties in meteorological conditions, with domain-integrated root-mean-square errors of 100 m for the nocturnal boundary layer (6–12 UTC) to 250 m in the convective boundary layer (0 UTC). The wind errors overall are slightly smaller than but nevertheless highly consistent with the errors in Meng and Zhang (2008b; supporting information Figure S3). Meng and Zhang (2008b) found that their uncertainties in the *u* and *v* components of the wind are realistic when verifying against observations, which indicates that the transport errors in our experiment are reasonable.

Next, we focus on uncertainties in simulated atmospheric CO_2 mole fractions. The temporal evolutions of vertically and domain-integrated transport, flux, and background uncertainties are shown in Figure 2a. Uncertainties in transport or CO_2 fluxes quickly degrade the perfect atmospheric CO_2 initial conditions. The uncertainties saturate after only 12 hr and maintain a consistent mean daily magnitude over time, except for an apparent increase on 9 July and a decrease on 30 July, which are due to changes in the weekly optimized CO_2 fluxes in CT-NRT. The vertically integrated transport and flux uncertainties reflect mainly the large uncertainties close to the surface (Figure 2c). There is a distinct diurnal cycle in both transport and flux uncertainties, with large peaks in the early mornings local time related to the stratification of the nocturnal boundary layer. The diurnal variation in transport uncertainties is not seen in column-averaged CO_2 (XCO_2; see Figures 2g and 2h), suggesting that the large transport uncertainties in the nocturnal boundary layer are mostly due to uncertainties in vertical mixing. The near-surface flux uncertainties show a secondary and smaller peak in the afternoon local time (Figure 2d) due to the strong photosynthetic uptake of CO_2 in summer, which is also reflected in XCO_2 (Figure 2h).

Flux uncertainties in the free troposphere above the boundary layer take about a week to saturate (Figure 2e). There is not much CO_2 error growth due to erroneous CO_2 surface fluxes beyond 1 week because air that has

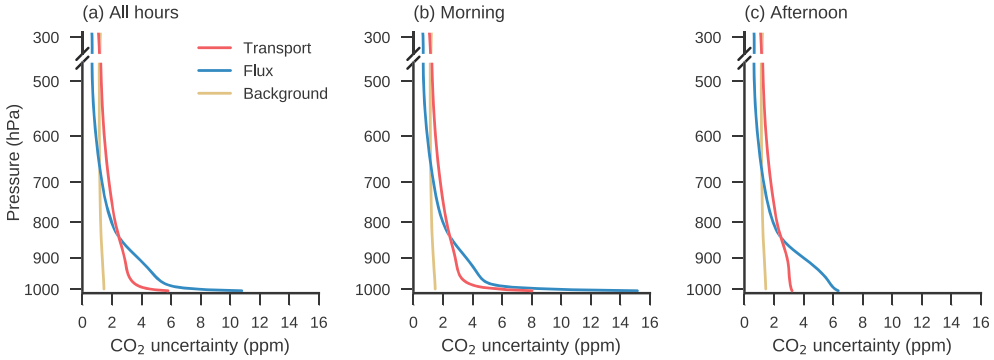

Figure 3. Vertical distribution of time- and domain-integrated uncertainties in CO_2 mole fractions in terms of one ensemble standard deviation for (a) all hours, (b) late night to early morning hours (6–12 UTC), and (c) afternoon hours (18–0 UTC). The vertical axis is the nominal pressure level (log scale) based on a sea-level pressure of 1013.25 hPa.

been affected by the regional fluxes is continuously advected out of the limited-area domain. As a result of this loss of flux signals through the lateral boundaries, transport and background uncertainties have a larger influence in the free troposphere than flux uncertainties in our experiments. Moreover, our results suggest that CO_2 errors due to transport uncertainties or background uncertainties are significantly correlated vertically and therefore do not cancel out when averaged vertically; thus, these error sources can considerably influence XCO_2 estimates (Figure 2g).

Figure 3 shows the vertical distribution of time- and domain-integrated CO_2 uncertainties. For this and all subsequent time integrations we excluded the first week to account for the spin-up time of uncertainties.

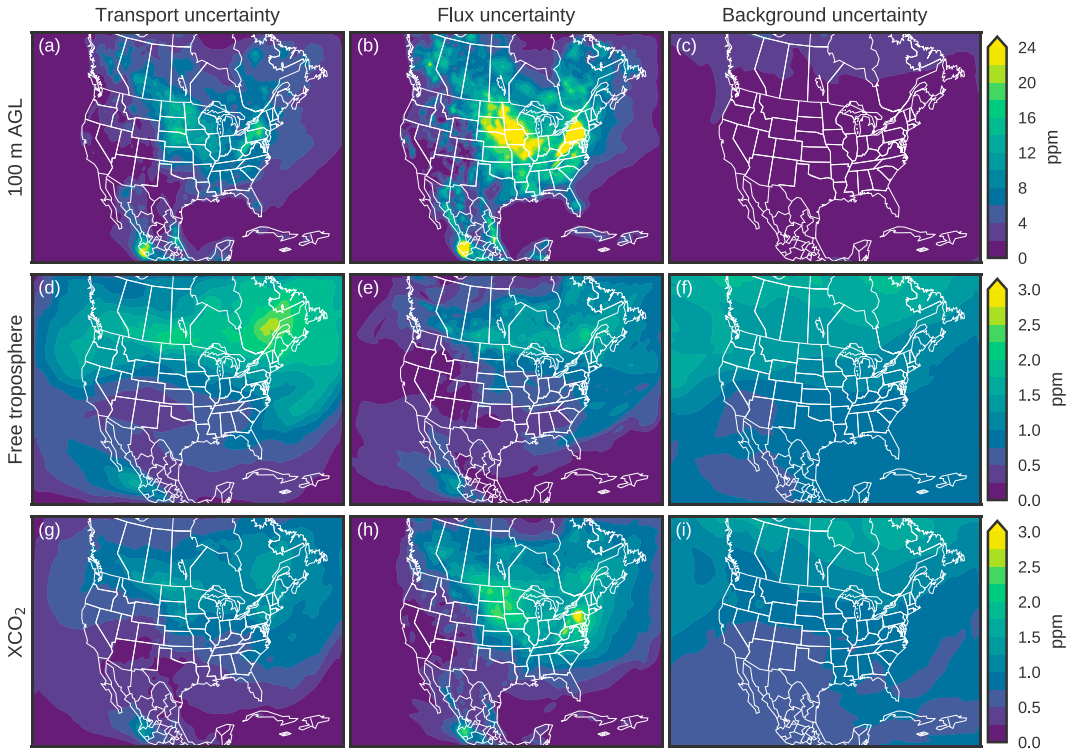

Figure 4. Horizontal distribution of time-integrated uncertainties in CO_2 mole fractions (ppm) in terms of one ensemble standard deviation for transport uncertainties (left column), flux uncertainties (middle column), and background uncertainties (right column) for (a–c) CO_2 at 100 m above ground level (AGL), (d–f) vertically integrated CO_2 uncertainties in the free troposphere, and (g–i) column-averaged CO_2.

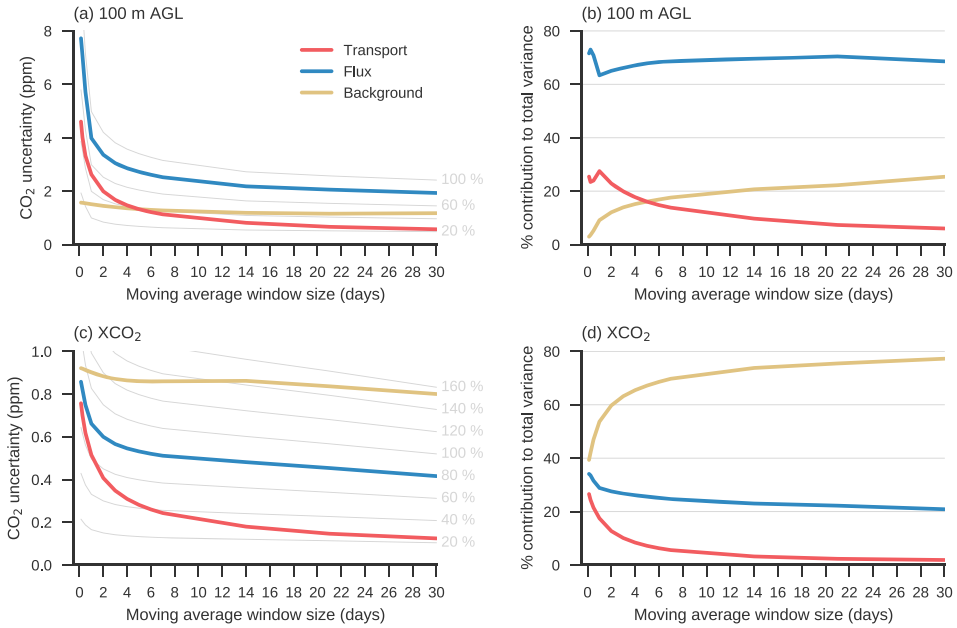

Figure 5. Time- and domain-integrated uncertainties in CO_2 mole fractions in terms of one ensemble standard deviation when the CO_2 mole fractions are averaged over varying time windows. Actual CO_2 uncertainties (left column) and relative uncertainty contributions from the different error sources to the total variance assuming that the errors are independent (right column) for (a, b) CO_2 at 100 m above ground level (AGL) and (c, d) column-averaged CO_2. The gray lines in the left column indicate the flux uncertainties for different relative flux errors, obtained by scaling the 80% flux uncertainties from the flux sensitivity experiment.

Flux and transport uncertainties are largest close to the surface, as expected, while background uncertainties vary only weakly across vertical model levels. In the afternoon, when atmospheric CO_2 mole fractions in the boundary layer are typically representative of larger areas, the time- and domain-integrated flux uncertainties near the surface are almost twice as large as the transport uncertainties (Figure 3c), which suggests that near-surface CO_2 observations are primarily influenced by flux uncertainties (roughly four times larger variance than transport uncertainties) during this time.

Figure 4 shows the horizontal distributions of time-integrated CO_2 uncertainties. Because we used scaling factors to perturb the CO_2 surface fluxes, the flux uncertainties at 100 m above ground level are large in areas with strong fluxes (Figure 4b). The same areas tend to have large near-surface transport uncertainties (Figure 4a) due to the stronger horizontal and vertical CO_2 gradients created by the fluxes. Background uncertainties are comparably small near the surface (Figure 4c) but considerable in the free troposphere (Figure 4f) and for XCO_2 (Figure 4i). Much of the background uncertainties originate from the northern lateral boundaries (supporting information Figure S4). In the free troposphere, transport and flux uncertainties are larger in the northern part of the domain where there is more extratropical cyclone activity (Figures 4d and 4e). Uncertainties in XCO_2 (Figures 4g–4i) reflect the joint uncertainties at both the surface and in the free troposphere.

Finally, we quantify how transport, flux, and background uncertainties vary from subdaily to monthly timescales. To this end, we calculated moving averages of 3-hourly instantaneous atmospheric CO_2 mole fractions over different-length time windows and then calculated the mean domain-integrated uncertainties for the different time-averaged CO_2 fields. Figure 5 shows the CO_2 uncertainties for the different error components with varying averaging window size. At 100 m above ground level, transport and flux uncertainties exhibit a similar exponential decay with increasing averaging window size, while background uncertainties decrease by only a small amount when time averaged (Figure 5a). The magnitude of near-surface flux uncertainties initially decreases fastest with increasing window length when averaged over the daily cycle. As the analysis is extended to longer averaging windows, transport uncertainties decrease until they are the smallest of the error components (Figure 5b). These results suggest that background uncertainties have the

largest spatial and temporal error correlation structures, while transport uncertainties have smaller error correlation length scales than flux uncertainties. For instantaneous CO_2 at 100 m above ground level, the transport uncertainties in our experiment yield a similar domain-integrated ensemble spread in CO_2 mole fractions as 48% uncertainties in 3-hourly surface fluxes (see gray lines in Figure 5a). When averaged over 1 week the transport uncertainties correspond to about 36% relative uncertainties in CO_2 fluxes, and over the whole month the correspondence asymptotes to 24%.

In terms of time- and domain-integrated uncertainties in XCO_2, the influence of background uncertainties exceeds the other uncertainty sources at all timescales in our month-long experiments (Figure 5c). Further, the relative importance of background uncertainties increases at longer timescales (Figure 5d). Although local XCO_2 estimates can be more sensitive to CO_2 fluxes in the close vicinity of strong sources and sinks (Figure 4h), these results indicate that background uncertainties can be a major error source for XCO_2 estimates, especially when considering longer timescales.

4. Concluding Remarks

In this study, we quantified and contrasted uncertainties in simulated atmospheric CO_2 mole fractions in a regional model from three error sources: atmospheric transport errors, errors in CO_2 surface fluxes, and errors in CO_2 background mole fractions from the lateral boundaries. Transport uncertainties were derived from an ensemble of simulations with perturbed meteorological fields. The uncertainties in meteorological variables reflect the current capabilities of estimating meteorological conditions based on the operational network of rawinsonde observations and state-of-the-art data assimilation methods. It is possible that meteorological uncertainties can be further reduced by assimilating, for example, satellite observations, but considering that we ignored other error sources in our idealized experimental setup (e.g., model error, representation error, and biased meteorological observations), we are likely underestimating transport errors, which is also indicated by our overall smaller wind errors compared with Meng and Zhang (2008b). Nevertheless, we found that transport uncertainties due to only imperfect meteorological initial and boundary conditions significantly affect forward simulations of CO_2 mole fractions in our experiment.

The fluxes in our flux sensitivity experiment were perturbed by applying ecoregion-specific scaling factors to the fluxes following the methodology used by, for example, the CarbonTracker system. Although these flux error covariances are highly simplified, they correspond to the flux uncertainties that are presently used in some inversion systems including CarbonTracker. In our study we kept the flux scaling factors constant over the whole simulation period, but despite this long-term persistence in flux errors, the fluxes leave a limited footprint on CO_2 mole fractions in our regional model because the flux signals are advected out of the limited-area domain. One caveat of our modeling experiments is that the convective parameterization scheme we used does not include tracer transport and we therefore most likely underestimate atmospheric flux uncertainties due to neglected convective transport, especially in the southern part of the domain. Nonetheless, we do not expect the inclusion of convective transport to change the conclusions of this study. Uncertainties in CO_2 lateral boundary conditions resulted in persistent differences in the CO_2 background that may arise from biases in the global systems, or from systematic errors in the interpolation of the global CO_2 mole fractions to the regional lateral boundary conditions.

The findings of this study have several implications for regional atmospheric inversions. Because erroneous CO_2 fluxes do not lead to long-term accumulation of errors in CO_2 mole fractions in a limited-area domain, regional inversions need to take into account the relatively large transport and background uncertainties when assimilating free tropospheric CO_2 observations, including aircraft measurements outside the boundary layer and column-averaged XCO_2 from satellites. At short timescales the flux signals in near-surface CO_2 mole fraction estimates are degraded by transport uncertainties, which have similar spatial and temporal patterns as CO_2 uncertainties due to erroneous fluxes. At longer timescales transport uncertainties are partially averaged out but compensated by uncertainties in CO_2 background mole fractions. In our experiments, background uncertainties exceed transport uncertainties when the averaging window size exceeds 5 days for CO_2 observations at 100 m above ground level. Finally, we found that CO_2 lateral boundary conditions from different global modeling systems produce persistent differences in CO_2 background mole fractions, and it may be advantageous for regional inversions to also continually optimize the CO_2 background as part of the inversion procedure.

Acknowledgments
This work was funded by the National Aeronautics and Space Administration (NASA) Atmospheric Carbon and Transport (ACT)-America Mission. ACT-America is a NASA Earth Venture Suborbital 2 project funded by NASA's Earth Science Division (Grant NNX15AG76G to Penn State). The data used for providing initial and boundary conditions are publicly available and include CarbonTracker Near-Real Time v2017, provided by the National Oceanic and Atmospheric Administration (NOAA; ftp://aftp.cmdl.noaa.gov/products/carbontracker/co2/CT-NRT.v2017/), and ERA-Interim, provided by the Research Data Archive (RDA) of the Computational and Information Systems Laboratory at the National Center for Atmospheric Research (NCAR). Computing was performed at the Texas Advanced Computing Center (TACC) where the modeling data output used in this study are archived. NCAR and TACC are supported by grants from the National Science Foundation. The locations of rawinsonde observations were obtained from the National Centers for Environmental Prediction (NCEP) Meteorological Assimilation Data Ingest System (MADIS; https://madis.ncep.noaa.gov). We thank Yue (Michael) Ying, Xinxin Ye, and Yonghui Weng for technical support, and two anonymous reviewers for helpful comments.

References

Basu, S., Miller, J., & Lehman, S. (2016). Separation of biospheric and fossil fuel fluxes of CO_2 by atmospheric inversion of CO_2 and $14CO_2$ measurements: Observation system simulations. *Atmospheric Chemistry and Physics*, *16*, 5665–5683. https://doi.org/10.5194/acp-16-5665-2016

Chevallier, F., Feng, L., Bösch, H., Palmer, P. I., & Rayner, P. J. (2010). On the impact of transport model errors for the estimation of CO_2 surface fluxes from GOSAT observations. *Geophysical Research Letters*, *37*, L21803. https://doi.org/10.1029/2010GL044652

Chevallier, F., Palmer, P. I., Feng, L., Boesch, H., O'Dell, C. W., & Bousquet, P. (2014). Toward robust and consistent regional CO_2 flux estimates from in situ and spaceborne measurements of atmospheric CO_2. *Geophysical Research Letters*, *41*, 1065–1070. https://doi.org/10.1002/2013GL058772

Ciais, P., Rayner, P., Chevallier, F., Bousquet, P., Logan, M., Peylin, P., & Ramonet, M. (2010). Atmospheric inversions for estimating CO_2 fluxes: Methods and perspectives. *Climatic Change*, *103*(1-2), 69–92. https://doi.org/10.1007/s10584-010-9909-3

Dee, D. P., Uppala, S. M., Simmons, A. J., Berrisford, P., Poli, P., Kobayashi, S., et al. (2011). The ERA-Interim reanalysis: Configuration and performance of the data assimilation system. *Quarterly Journal of the Royal Meteorological Society*, *137*(656), 553–597. https://doi.org/10.1002/qj.828

Díaz-Isaac, L. I., Lauvaux, T., & Davis, K. J. (2018). Impact of physical parameterizations and initial conditions on simulated atmospheric transport and CO_2 mole fractions in the US Midwest. *Atmospheric Chemistry and Physics*, *18*(20), 14,813–14,835. https://doi.org/10.5194/acp-18-14813-2018

Dudhia, J. (1988). Numerical study of convection observed during the winter monsoon experiment using a mesoscale two-dimensional model. *Journal of the Atmospheric Sciences*, *46*(20), 3077–3107. https://doi.org/10.1175/1520-0469(1989)046<3077:NSOCOD>2.0.CO;2

Engelen, R. J., Denning, A. S., & Gurney, K. R. (2002). On error estimation in atmospheric CO_2 inversions. *Journal of Geophysical Research*, *107*(D22), 10–13. https://doi.org/10.1029/2002JD002195

Enting, I. G. (2002). *Inverse problems in atmospheric constituent transport*. Cambridge: Cambridge University Press. https://doi.org/10.1017/CBO9780511535741

Evensen, G. (1994). Sequential data assimilation with a nonlinear quasi-geostrophic model using Monte Carlo methods to forecast error statistics. *Journal of Geophysical Research*, *99*(C5), 10,143–10,162. https://doi.org/10.1029/94JC00572

Gaspari, G., & Cohn, S. E. (1999). Construction of correlation functions in two and three dimensions. *Quarterly Journal of the Royal Meteorological Society*, *125*(554), 723–757. https://doi.org/10.1002/qj.49712555417

Gloor, M., Fan, S. M., Pacala, S., Sarmiento, J., & Ramonet, M. (1999). A model-based evaluation of inversions of atmospheric transport, using annual mean mixing ratios, as a tool to monitor fluxes of nonreactive trace substances like CO_2 on a continental scale. *Journal of Geophysical Research*, *104*(D12), 14,245–14,260. https://doi.org/10.1029/1999JD900132

Grell, G. A., Peckham, S. E., Schmitz, R., McKeen, S. A., Frost, G., Skamarock, W. C., & Eder, B. (2005). Fully coupled "online" chemistry within the WRF model. *Atmospheric Environment*, *39*(37), 6957–6975. https://doi.org/10.1016/j.atmosenv.2005.04.027

Gurney, K. R., Law, R. M., Denning, A. S., Rayner, P. J., Baker, D., Bousquet, P., et al. (2002). Towards robust regional estimates of CO_2 sources and sinks using atmospheric transport models. *Nature*, *415*(6872), 626–630. https://doi.org/10.1038/415626a

Hong, S. Y., Dudhia, J., & Chen, S. H. (2004). A revised approach to ice microphysical processes for the bulk parameterization of clouds and precipitation. *Monthly Weather Review*, *132*(1), 103–120. https://doi.org/10.1175/1520-0493(2004)132<0103:ARATIM>2.0.CO;2

Houtekamer, P. L., & Zhang, F. (2016). Review of the ensemble Kalman filter for atmospheric data assimilation. *Monthly Weather Review*, *144*(12), 4489–4532. https://doi.org/10.1175/MWR-D-15-0440.1

Kain, J. S. (2004). The Kain–Fritsch convective parameterization: An update. *Journal of Applied Meteorology*, *43*(1), 170–181. https://doi.org/10.1175/1520-0450(2004)043<0170:TKCPAU>2.0.CO;2

Kang, J. S., Kalnay, E., Miyoshi, T., Liu, J., & Fung, I. (2012). Estimation of surface carbon fluxes with an advanced data assimilation methodology. *Journal of Geophysical Research*, *117*, D24101. https://doi.org/10.1029/2012JD018259

Lauvaux, T., Pannekoucke, O., Sarrat, C., Chevallier, F., Ciais, P., Noilhan, J., & Rayner, P. J. (2009). Structure of the transport uncertainty in mesoscale inversions of CO_2 sources and sinks using ensemble model simulations. *Biogeosciences*, *6*(6), 1089–1102. https://doi.org/10.5194/bg-6-1089-2009

Lin, J. C., & Gerbig, C. (2005). Accounting for the effect of transport errors on tracer inversions. *Geophysical Research Letters*, *32*, L01802. https://doi.org/10.1029/2004GL021127

Liu, J., Bowman, K. W., Lee, M., Henze, D. K., Bousserez, N., Brix, H., et al. (2014). Carbon monitoring system flux estimation and attribution: Impact of ACOS-GOSAT XCO2 sampling on the inference of terrestrial biospheric sources and sinks. *Tellus B*, *66*(1), 22486. https://doi.org/10.3402/tellusb.v66.22486

Liu, J., Fung, I., Kalnay, E., & Kang, J. S. (2011). CO_2 transport uncertainties from the uncertainties in meteorological fields. *Geophysical Research Letters*, *38*, L12808. https://doi.org/10.1029/2011GL047213

Lorenz, E. N. (1963). Deterministic nonperiodic flow. *Journal of the Atmospheric Sciences*, *20*(2), 130–141. https://doi.org/10.1175/1520-0469(1963)020<0130:DNF>2.0.CO;2

Meng, Z., & Zhang, F. (2007). Tests of an ensemble Kalman filter for mesoscale and regional-scale data assimilation. Part II: Imperfect model experiments. *Monthly Weather Review*, *135*(4), 1403–1423. https://doi.org/10.1175/MWR3352.1

Meng, Z., & Zhang, F. (2008a). Tests of an ensemble Kalman filter for mesoscale and regional-scale data assimilation. Part III: Comparison with 3DVAR in a real-data case study. *Monthly Weather Review*, *136*(2), 522–540. https://doi.org/10.1175/2007MWR2106.1

Meng, Z., & Zhang, F. (2008b). Tests of an ensemble Kalman filter for mesoscale and regional-scale data assimilation. Part IV: Comparison with 3DVAR in a month-long experiment. *Monthly Weather Review*, *136*(10), 3671–3682. https://doi.org/10.1175/2008MWR2270.1

Miller, S. M., Hayek, M. N., Andrews, A. E., Fung, I., & Liu, J. (2015). Biases in atmospheric CO_2 estimates from correlated meteorology modeling errors. *Atmospheric Chemistry and Physics*, *15*(5), 2903–2914. https://doi.org/10.5194/acp-15-2903-2015

Mlawer, E. J., Taubman, S. J., Brown, P. D., Iacono, M. J., & Clough, S. A. (1997). Radiative transfer for inhomogeneous atmospheres: RRTM, a validated correlated–k model for the longwave. *Journal of Geophysical Research*, *102*(D14), 16,663–16,682. https://doi.org/10.1029/97JD00237

Nakanishi, M., & Niino, H. (2006). An improved Mellor–Yamada level-3 model: Its numerical stability and application to a regional prediction of advection fog. *Boundary Layer Meteorol.*, *119*(2), 397–407. https://doi.org/10.1007/s10546-005-9030-8

National Research Council (2010). *Verifying greenhouse gas emissions: Methods to support international climate agreements*. Washington, DC: The National Academies Press. https://doi.org/10.17226/12883

Olson, J. S., Watts, J. A., & Allison, L. J. (1985). Major world ecosystem complexes ranked by carbon in live vegetation: A database (NDP-017). Oak Ridge, TN: Carbon Dioxide Information Center, Oak Ridge Laboratory.

Peters, W., Jacobson, A. R., Sweeney, C., Andrews, A. E., Conway, T. J., Masarie, K., et al. (2007). An atmospheric perspective on North American carbon dioxide exchange: CarbonTracker. *Proceedings of the National Academy of Sciences of the United States of America*, *104*(48), 18,925–18,930. https://doi.org/10.1073/pnas.0708986104

Peylin, P., Law, R. M., Gurney, K. R., Chevallier, F., Jacobson, A. R., Maki, T., et al. (2013). Global atmospheric carbon budget: Results from an ensemble of atmospheric CO_2 inversions. *Biogeosciences*, *10*, 6699–6720. https://doi.org/10.5194/bg-10-6699-2013

Polavarapu, S. M., Neish, M., Tanguay, M., Girard, C., de Grandpré, J., Semeniuk, K., et al. (2016). Greenhouse gas simulations with a coupled meteorological and transport model: The predictability of CO_2. *Atmospheric Chemistry and Physics*, *16*(18), 12,005–12,038. https://doi.org/10.5194/acp-16-12005-2016

Schuh, A. E., Baker, D. F., & Jacobson, A. R. (2015). GEOS-Chem-CarbonTracker.

Skamarock, W., Klemp, J., Dudhia, J., Gill, D., Barker, D., Duda, M., et al. (2008). A description of the advanced research WRF Version 3 (NCAR technical note). Boulder, CO: Mesoscale and Microscale Meteorology Division National Center for Atmospheric Research. https://doi.org/10.5065/D68S4MVH

Stephens, B. B., Gurney, K. R., Tans, P. P., Sweeney, C., Peters, W., Bruhwiler, L., et al. (2007). Weak northern and strong tropical land carbon uptake from vertical profiles of atmospheric CO_2. *Science*, *316*(5832), 1732–1735. https://doi.org/10.1126/science.1137004

Tans, P. P., Fung, I. Y., & Takahashi, T. (1990). Observational constrains on the global atmospheric CO_2 budget. *Science*, *247*(4949), 1431–1438. https://doi.org/10.1126/science.247.4949.1431

Tewari, M., Chen, F., Wang, W., Dudhia, J., LeMone, M. A., Mitchell, K., et al. (2004). Implementation and verification of the unified NOAH land surface model in the WRF model. In *20th conference on weather analysis and forecasting/16th conference on numerical weather prediction*, (pp. 11–15). Seattle.

Weng, Y., & Zhang, F. (2012). Assimilating airborne doppler radar observations with an ensemble Kalman filter for convection-permitting hurricane initialization and prediction: Katrina (2005). *Monthly Weather Review*, *140*(3), 841–859. https://doi.org/10.1175/2011MWR3602.1

Weng, Y., & Zhang, F. (2016). Advances in convection-permitting tropical cyclone analysis and prediction through EnKF assimilation of reconnaissance aircraft observations. *Journal of the Meteorological Society of Japan*, *94*(4), 345–358. https://doi.org/10.2151/jmsj.2016-018

Zhang, F., Minamide, M., & Clothiaux, E. E. (2016). Potential impacts of assimilating all-sky infrared satellite radiances from GOES-R on convection-permitting analysis and prediction of tropical cyclones. *Geophysical Research Letters*, *43*, 2954–2963. https://doi.org/10.1002/2016GL068468

Zhang, F., Minamide, M., Nystrom, R. G., Chen, X., Lin, S. J., & Harris, L. M. (2019). Improving Harvey forecasts with next-generation weather satellites. *Bulletin of the American Meteorological Society*. https://doi.org/10.1175/BAMS-D-18-0149.1

Zhang, F., Snyder, C., & Sun, J. (2004). Impacts of initial estimate and observation availability on convective-scale data assimilation with an ensemble Kalman filter. *Monthly Weather Review*, *132*(5), 1238–1253. https://doi.org/10.1175/1520-0493(2004)132<1238:IOIEAO>2.0.CO;2

Zhang, F., Weng, Y., Gamache, J. F., & Marks, F. D. (2011). Performance of convection-permitting hurricane initialization and prediction during 2008-2010 with ensemble data assimilation of inner-core airborne Doppler radar observations. *Geophysical Research Letters*, *38*, L15810. https://doi.org/10.1029/2011GL048469

Zhang, F., Weng, Y., Sippel, J. A., Meng, Z., & Bishop, C. H. (2009). Cloud-resolving hurricane initialization and prediction through assimilation of doppler radar observations with an ensemble Kalman filter. *Monthly Weather Review*, *137*(7), 2105–2125. https://doi.org/10.1175/2009MWR2645.1